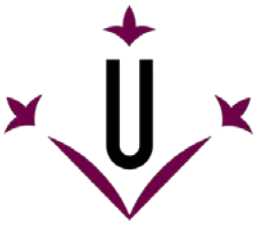

Free Indium concentration determined with AGNES

Marjan H. Tehrani, Encarna Companys*, Angela Dago, Jaume Puy and Josep Galceran

Departament de Química. Universitat de Lleida, and AGROTECNIO, Rovira Roure 191, 25198 Lleida, Catalonia, Spain

* corresponding author ecompanys@quimica.udl.cat

Abstract

Indium is increasingly used in electronic devices, from which it can be mobilized towards environmental compartments. Speciation of In in waters is important for its direct ecotoxicological effects, as well as for the fate of this element in the environment (e.g. fluxes from or towards sediments). Free indium concentrations in the environment can be extremely low due to hydrolysis, especially important in trivalent cations, to precipitation and to complexation with different ligands. In this work, the free indium concentration (which is a toxicologically and geochemically relevant fraction) in aqueous solutions at pH 3 has been measured with an adapted version of the electroanalytical technique AGNES (Absence of Gradients and Nernstian Equilibrium Stripping). Speciation measurements in mixtures of indium with the ligands NTA (nitrilotriacetic acid) and oxalate indicate that the values of their stability constants in the NIST46.6 database are less adequate than those published in some more recent literature. The extraordinary lability and mobility of In-oxalate complexes allow the measuring of free indium concentrations below nanomol/liter in just 25 s of deposition time.

Keywords: bioavailability, speciation, In(III), complexation, free metal ion, technology critical element

Highlights

- AGNES technique can measure free indium concentrations in aqueous solutions

- A specific calibration procedure has been developed for indium
- NIST46.6 stability constant values for In-complexes with oxalate or NTA are not optimal.
- High lability and mobility of In-oxalate complexes lead to fast measurements

1. Introduction

Ecotoxicological paradigms such as the Free Ion Activity Model (FIAM) or the Biotic Ligand Model (BLM) attribute a key role to the free metal ion concentration (or activity) (Paquin et al., 2002). Suitable analytical methods are therefore needed, for a variety of elements, to target this specific fraction of their total concentration.

Indium is a critical element present in a huge number of electronic devices (Abbas and Amer, 2013;Chung and Lee, 2012;Wood and Samson, 2006), from which it will eventually leach towards environmental waters and other compartments (White and Hemond, 2012;Zimmermann et al., 2013). To understand these fluxes from the anthroposphere to the hydrosphere, lithosphere and biosphere, the relevant chemical properties of this poorly-studied element have to be adequately elucidated. For instance, the large hydrolysis processes of indium (e.g. an increase by 0.1 units in the pH of a solution in equilibrium with precipitated $In(OH)_3$ decreases the free concentration by a factor of 2) are key to explain the transfer from some natural waters to the sediments (Nosal-Wiercinska, 2010;White et al., 2017). Moreover, hydrolysis also hinders the accurate study of its speciation with most conventional techniques and, so, there are many unresolved aspects of the behaviour of indium in a number of systems (Chung and Lee, 2012;Tuck, 1983). In particular, values of the reported stability constants of indium with most ligands are remarkably uncertain (Tuck, 1983).

Total indium concentrations in natural waters have been reported to be, generally, extremely low. Using mass spectrometry, Alibo et al. (1998) reported total

concentrations of indium in the Pacific and Atlantic oceans in the range of 0.06 to 0.15 pmol/kg and 0.6 to 1.5 pmol/kg respectively, while river and estuarine waters were in the range 0.01 to 15 pmol/kg. A recent review (White and Hemond, 2012) concluded concentrations of indium in oceans from 0.006 to 0.5 ng L^{-1} and from 0.13 to 15 pg L^{-1} for some freshwaters. The concentration of dissolved indium (White et al., 2017) could reach 6 to 29 μg/L in streams influenced by acid mine drainage (pH around 3).

Several proposals for measuring free indium concentrations (i.e. the free concentrations of the hexaaquo complex) have been reported, including Ion Selective Electrodes (Abbas and Amer, 2013;Gupta et al., 2010) or molecularly imprinted polymer sensors (Zhang et al., 2015), but their limit of quantification (around 10^{-7} mol L^{-1}) is still relatively modest.

AGNES (Absence of Gradients and Nernstian Equilibrium Stripping) (Galceran et al., 2004) is an emerging electroanalytical technique designed to determine free metal ion concentrations in solutions. Specific studied systems with environmental interest include seawaters (Diaz-de-Alba et al., 2014;Galceran et al., 2007), estuarine waters (Pearson et al., 2016), river waters (Parat et al., 2015;Zavarise et al., 2010), dispersions of nanoparticles (Adam et al., 2014;David et al., 2012;Domingos et al., 2008;Mu et al., 2014;Vale et al., 2015), quantum dots (Domingos et al., 2011), clay minerals dispersions (Rotureau, 2014), extracts of soils (Chito et al., 2012), humic acids solutions (Companys et al., 2007;Puy et al., 2008), etc. (see recent review (Galceran et al., 2014)). Although solid electrodes of Bi and Au have been able to determine free concentrations of Pb (Rocha et al., 2015) and Cu (Domingos et al., 2016), respectively, the typical implementation of AGNES with mercury electrodes requires amalgamating elements such as Zn, Cd, Pb or Sn. Given that indium is also an amalgamating element with a

negative standard redox potential, it can be tackled with AGNES and conventional Hg electrodes.

The aim of this work is to show how AGNES can measure free indium concentration, [In^{3+}]. For toxicological and geochemical studies, the free ion concentration is a very relevant (even if sometimes small) fraction of the total dissolved concentration. This is the first application of AGNES to a trivalent ion. pH 3 is chosen here to avoid any complication from hydrolysis (Nosal-Wiercinska, 2010;White et al., 2017), for which conflicting formation constants have been reported (Alekseev et al., 2013;Tuck, 1983). This pH is relevant for acid mine drainages where high In concentrations have been reported (Nosal-Wiercinska, 2010;White et al., 2017). Speciation capability will be assessed with a ligand (NTA, nitrilotriacetic acid) forming a relatively inert complex and another one (oxalate) forming a labile one. In-NTA is also interesting for its application, in radiodiagnostic medicine (Biver et al., 2008), as vector of isotopes In-111 and In-113 to transferrin (implying iron substitution).

2. Experimental

2.1 Reagents

Indium solutions were prepared by dilution from a 1000 mg L^{-1} stock solution (Fluka, indium standard for ICP). NTA and potassium oxalate monohydrate (both Fluka, analytical grade) were used as ligands. Potassium nitrate was used as the inert supporting electrolyte at 0.1 mol L^{-1} (for all experiments) and prepared from solid KNO_3 (Fluka, TraceSelect). KOH and HNO_3 0.1 mol L^{-1} (Fluka) were used to adjust the pH of the solutions.

Ultrapure water (Synergy UV purification system Millipore) was used in all experiments. Purified water saturated N_2 (purity ≥ 99.999%) was used for deaeration and blanketing the solutions.

2.2 Instrumentation and procedures

Voltammetric measurements were carried out with Autolab PGSTAT10 and PGSTAT101 potentiostats attached to Metrohm 663 VA Stands. All experiments were performed using GPES 4.9.007 (Eco Chemie) and NOVA 1.11 (Metrohm Autolab) software.

The working electrode was a Metrohm Hanging Mercury Drop Electrode (HMDE). Glassy carbon was used as the auxiliary electrode and the reference electrode was double-junction Ag/AgCl/3mol L^{-1} KCl with KNO_3 0.1 mol L^{-1} in the salt bridge. A glass jacketed cell was used in all the experiments and thermostated at 25.0°C. A glass combined electrode (Crison, 5209) was attached to an Orion Dual Star ion analyzer (Thermo) and introduced in the cell to measure and, accordingly, control the pH.

Purging with N_2 was necessary not only to spare a large signal from oxygen reduction, but also to avoid dramatic pH increases close to the electrode surface which would lead to indium hydrolysis (Aguilar et al., 2013a;Statsyuk and Dergacheva, 1998).

Differential Pulse Polarography (DPP) was used to have an initial estimate of the (deposition) potential to be applied in AGNES for a desired gain (i.e. accumulation factor) compensating any drift from the reference electrode. For DPP experiments, the largest stand drop (labelled "3" which according to the catalogue corresponds to a radius r_0 = 203 μm) has been used in order to be able to apply an expression, valid for planar geometry, to the DPP peak potential (Bard and Faulkner, 2001; Galceran et al., 2004). For the "short" DPP variant the drop lifetime was t_d=0.1 s, while for the "long" DPP was t_d=1 s; the scan rate was 4.5 mV/s and 0.45 mV/s, respectively. In both DPPs, the typical initial potential was -0.4 V and the final potential was -0.6 V; a modulation amplitude of 49.95 mV and a pulse time t_p=50 ms were applied.

To assess indium reversibility (i.e. the fast reaching of equilibrium conditions -ruled by Nernst equation- between In^0 and In^{3+} at the electrode surface) in the conditions of this work, Cyclic Voltammograms (CV) were performed between -0.1 V and -0.8 V with a scan rate of 10 mV/s. More details on the ancillary techniques (DPP and CV) and on AGNES can be found in the Supplementary Material (SM).

We faced some difficulties while we were doing the speciation measurements with indium. The capillar of the mercury drop electrode was blocked more often than usual and we had also some irreproducibilities.

2.3 AGNES principles applied to indium analysis

AGNES is a stripping technique with two stages: deposition (accumulation in the amalgam) and stripping.

The deposition stage in AGNES lasts until a special situation of equilibrium is reached. Two conditions must be met: i) the ratio (called gain, Y) between the concentration in the amalgam and the free ion concentration in the solution is ruled by Nernst equation:

$$Y = \frac{\left[\mathrm{In}^0\right]}{\left[\mathrm{In}^{3+}\right]} = \exp\left[-\frac{3F}{RT}\left(E_1 - E^{0'}\right)\right] \quad (1)$$

where F is the Faraday constant, R the gas constant, T the temperature, E_1 is the applied deposition potential and $E^{o'}$ is the standard formal potential of the redox couple; and ii) there are no gradients in the concentration profiles of the involved species (e.g. no fluxes of In^0, In^{3+}, etc.). In the simplest variant for the deposition stage, denoted 1P (one pulse), the total duration of the deposition stage applying E_1 is t_1, whose last period is an equilibration, resting or "waiting" time, t_w, without stirring. The variant 2P (two pulses) contains an added initial sub-step (for a time $t_{1,a}$) during which the element is accumulated under diffusion limited conditions ($E_{1,a} << E_1$); the desired gain (via E_1) is

153 prescribed during $t_{1,b}$ (with stirring) and t_w (without stirring) (Companys et al., 2005).
154 More details on the 1P and 2P variants are given in the SM. The required deposition
155 times to reach equilibrium decrease with decreasing the radius of the drop (Huidobro et
156 al., 2007), so the smallest radius (drop 1 in Metrohm stand) is chosen for AGNES
157 experiments.
158 The stripping stage aims at the quantification of [In^0] in the amalgam. Several variants
159 have been developed (Galceran et al., 2014). The simplest and most popular variant,
160 AGNES-I, relies on measuring the faradaic intensity current at a certain stripping time.
161 However, the slight irreversibility of In (see section 3.1) suggests using the alternative
162 variant AGNES-Q which measures the stripped faradaic charge when a constant re-
163 oxidation potential (E_2) is applied for a sufficiently long stripping time (t_2). All the
164 accumulated moles of In^0 are now stripped away from the amalgam and, so, the
165 resulting faradaic charge (Q) is unaffected by any kinetics (provided full depletion of
166 In^0). Given the standard redox potentials of In (-0.510 V) and Pb (-0.317V), in this
167 work with indium, to avoid any interference of possible traces of Pb (Charalambous and
168 Economou, 2005;Esteban et al., 1992;Perez-Rafols et al., 2017), a fixed E_2=-0.450 V
169 (vs. Ag/AgCl) has been chosen for AGNES-Q. Some irreversible systems (e.g. those
170 with Zn) can also be analyzed with AGNES-I (Companys et al., 2005), because the
171 reoxidation potential can be sufficiently more positive than the standard redox potential
172 to overcome the irreversibility, without reaching a potential where the reoxidation
173 interference of other cations (e.g. Cd) occurs.
174
175 From Faraday's law and the equilibrium condition (1) reached by the end of the first
176 stage:

177 $$Q = 3FV_{Hg}[In^o] = 3FV_{Hg}Y[In^{3+}] \quad (2)$$

where V_{Hg} is the volume of the mercury electrode. The normalized proportionality factor (η_Q, obtained from a calibration in previous works with Zn, Cd and Pb (Parat et al., 2011) can be defined as:

$$\eta_Q = nFV_{Hg} \quad (3)$$

Combining eqns (2) and (3), one reaches the key equation for AGNES, which relates the analytical signal (faradaic charge in this case) with the free metal ion concentration:

$$Q = \eta_Q Y[In^{3+}] \quad (4)$$

The faradaic charge can be obtained by subtracting a synthetic blank (i.e. the solution with just background electrolyte) to the total charge (Galceran et al., 2014).

3. Results

3.1 Impact of irreversibility: specific calibration for In

For Zn, Cd or Pb, the potential (E_j) associated to a given gain (Y_j) can be computed from the peak potential of a Differential Pulse Polarogram (DPP) with the formula:

$$Y = \sqrt{\frac{D_{M^{n+}}}{D_{M^0}}} \exp\left[-\frac{nF}{RT}\left(E_1 - E_{peak} - \frac{\Delta E}{2}\right)\right] \quad (5)$$

where D_{M^0} is the diffusion coefficient for the reduced metal inside the amalgam, $D_{M^{n+}}$ is the diffusion coefficient for the free metal ion in solution, E_{peak} is the potential of the maximum obtained in a typical DPP (with the largest drop) and ΔE is the modulation amplitude of the DPP experiment. The expression for DPP assumes no complexation of the metal, so working at pH 3 limited the impact of the hydroxocomplexes of indium on the DPP peak potential. However, this formula assumes that the couple In^0/In^{3+} is behaving reversibly at the mercury electrode, while conflicting reports on the irreversibility of In (Almagro et al., 1977;Engblom and Ivaska, 1987;Guru and

Mahajan, 1976;Komatsu, 1973;Nosal-Wiercinska, 2010;Taher, 2000;Zelic et al., 1994) are known. The Cyclic Voltammogram (CV) shown in Fig. 1 exhibits its cathodic and anodic peaks at -0.502 and -0.479 V, respectively. So, their difference is 23 mV. According to the rule (see section 6.5.1 in (Bard and Faulkner, 2001), the expected difference in a reversible system should be:

$$\left|E_{\mathrm{pa}} - E_{\mathrm{pc}}\right| = \frac{RT}{nF}\ln(10) \approx \frac{59}{3}\,\mathrm{mV} \approx 19\,\mathrm{mV} \qquad (6)$$

This means that, in the CV timescale, the In couple is behaving quasi-reversibly. Thus, the (short term) irreversibility of indium prevents a direct accurate computation with the existing expression (5), so a new calibration procedure has been designed.

The key idea of the procedure is to fix η_{Q} according to eqn. (3) (instead of finding it as done with all other elements previously studied with AGNES). Using the radius of the drop 1 (which according to the catalogue corresponds to r_0= 141 μm), one obtains:

$$\eta_{\mathrm{Q}} = 0.0034\ \mathrm{C\ L\ mol^{-1}} \qquad (7)$$

One can calibrate by measuring the charge with AGNES for known free indium solutions applying a (judiciously chosen) fixed potential (called E_{calib}). Fig. 3 shows one of the calibrations used in this work. Taking into account eqn. (4), from the slope of the plot Q vs. [In^{3+}] and the fixed value of η_{Q} given by (7), one can find the gain actually applied during the calibration (called Y_{calib}) associated to the used E_{calib}.

As a rough initial guideline, and to avoid a blind trial-and-error process when starting with a new reference electrode, E_{calib} can be computed from an aimed gain by using an empirically modified version of equation (5) found in this work:

$$Y_{\text{estimated}} = 2.11\times\sqrt{\frac{D_{\text{In}^{3+}}}{D_{\text{In}^{0}}}}\exp\left[-\frac{3F}{RT}\left(E_1 - E_{\text{peak}} - \frac{\Delta E}{2}\right)\right] \quad (8)$$

where E_{peak} was determined from the "short" DPP (i.e. t_d=0.1s). In this work, the used diffusion coefficients were $D_{In^0} = 1.38\times10^{-9}$ m^2 s^{-1} (Galus, 1984) and $D_{In^{3+}} = 4.363\times10^{-10}$ m^2 s^{-1} (taken from table 1 in (Kariuki and Dewald, 1997), who reported this value from a previous research (Turnham, 1965)). Eqn. (8) provides a guideline (previous to the calibration) of the gain associated to a candidate E_{calib} because, from this gain, one can estimate the necessary deposition time (see section 3.2 below). After a succesful calibration, there is no longer need of any additional DPP run or use of eqn. (8), unless there is a dramatic change in the reference electrode, because (before a new calibration) one can use the estimate of the gain associated to the new E_{calib} from the previous calibration.

Fig. 3 is an example of such kind of calibrations, where the free indium concentration in the abscissae is just a fraction of the total dissolved indium (e.g. around 82% at pH 3, see details in Table SM-1 of the Supplementary Material).

Once the correspondence between E_{calib} and Y_{calib} is known, the necessary potential (E_j) to achieve any desired gain (Y_j) (and viceversa) can be computed with the aid of eqn. (1) as:

$$E_j = E_{\text{calib}} - \frac{RT}{3F}\ln\frac{Y_j}{Y_{\text{calib}}} \quad (9)$$

Even though the true values of η_Q and/or Y_j might be away from the computed ones in a calibration, the correction factor would cancel out because the same offset applies to the calibration and to the measurement.

The slight irreversibility which affects CV and DPP signals does not impact on the achievement of Nernstian equilibrium by the end of the first stage, just might delay it.

Moreover, the timescale of the relevant redox processes in experiments CV and DPP is short (of the order of seconds), while the deposition stage of AGNES is of the order of hundreds of seconds. On the other hand, if any irreversibility still had an effect, one would just see (in 1P variant) that longer deposition times lead to higher charges (because the response signal increases monotonously with t_1 as equilibrium is progressively approached as seen in Fig 4) and one would just lengthen t_1 until the stabilization of the analytical response. The irreversibility cannot affect the second stage of AGNES, either, because of the long re-oxidation step (t_2=50 s, ample time for diffusion inside the drop) stripping off all the material at a potential far away from equilibrium.

3.2 Time required to reach equilibrium

The attainment of equilibrium can be checked by performing a "trajectory" (time course or time profile): a set of experiments with a given gain and successively longer deposition times. When the charge stabilizes into a plateau or horizontal line (i.e. longer deposition times do not alter the measured charge), it is indicative of equilibrium. Before the plateau, lower values of charge are measured, which we term as undershoot values. Panel a) in Fig. 4 shows that the trajectories reach higher plateau values for higher gains, as expected from eqn. (4) (which only applies when equilibrium has been reached). Also, the time needed to reach the plateau increases with the gain. For previously studied divalent cations (Zn, Pb and Cd), the following rule (Galceran et al., 2010), when using the smallest radius (drop 1) of the stand, for the deposition time with stirring needed to reach a certain gain had been suggested:

$$t_1 - t_w = 7Y \qquad (10)$$

(where the resulting time is expressed in seconds). Previous formula has proved useful when a standard stirring speed ("6" in the stand, corresponding to 3000 min^{-1}) is in operation and when only the free metal contributes to the flux, i.e. for systems with just metal or with totally inert complexes.

The trajectories in panel a) of Fig. 4 have been re-plotted in panel b) in terms of a normalized charge, Q/Y, *vs.* a normalized deposition time with stirring $(t_1\text{-}t_w)/Y$. The collapse of trajectories into practically one master curve demonstrates two conclusions:

i) The rule for the required deposition time can be re-formulated, for indium, as:

$$t_1 - t_w = 10Y \qquad (11)$$

The slight increase in the deposition times required to reach AGNES equilibrium can be due to the described slight irreversibility of the In couple (as it is well known that irreversibility is more critical close to equilibrium situations) and to the lower diffusion coefficient of indium.

ii) The collapse of the plateaus of the normalized trajectories confirms the Nernstian behaviour: there is a direct proportionality between the gain and the accumulated charge (as also indicated by eqn. (4)).

3.3 Speciation measurements

3.3.1 In+NTA

A first checking of AGNES measuring the free metal ion concentration, when complexes are present, involved a ligand (NTA) typically forming inert complexes in voltammetric experiments (Alberti et al., 2007). Markers in Fig. 5 show the experimental results of the evolution of free indium in several mixtures with NTA (see Table 1), computing the plotted concentration from the average of the stabilized signals (typically at two different gains). AGNES 1P strategy with gains from 2 to 50 and deposition times $(t_1\text{-}t_w)$ up to 800 s was convenient until the total concentrations of NTA

298 and In were almost in the stoichiometric proportion 1:1. From this point of the titration
299 onwards, the required deposition times with the 1P strategy were very long, so AGNES
300 2P has been used. The point at $c_{T,NTA}$=12.14 μmol L^{-1} applying $Y_{1,a}=10^{10}$ produced large
301 overshoots, even with such a short $t_{1,a}$ as 1.5 s. It was observed that the accumulation
302 rate during the first substage declined with decreasing $Y_{1,a}$, so -to avoid large
303 overshoots- $Y_{1,a}=10^{8}$ was used for NTA concentrations higher than 12.14 μmol L^{-1}.
304 These lowest free indium concentrations involved gains in the range 5000 to 10^5 and
305 relaxation times ($t_{1,b}$) in the range 1000 to 2000 s (see Table 1).
306 As seen in Table 1, at the first additions (say until $c_{T,NTA}$=9.46 μmol L^{-1}), the decrease
307 in free In concentration measured with AGNES is practically equal to the amount of
308 added ligand, indicating a strong complexation between one In atom and one NTA
309 molecule (and perhaps other species such as H^+ or OH^-). When the stoichiometric
310 proportion 1:1 is reached, there is a sudden drop in the free In concentration (see Fig 5).
311 The use of the default NIST 46.6 (default database in the speciation program
312 VMINTEQ (Gustafsson, 2016)) for predicting the concentration is only acceptable
313 below the proportion 1:1. Using the stability constants of (Harris et al., 1994), the
314 agreement is practically the same as NIST46.6 for the first additions, but for the values
315 above the proportion 1:1, Harris' predicted free concentration is too low. The essential
316 difference between NIST's and Harris *et al*'s models is the value of the stability constant
317 for $InH(NTA)_2$ (see Table 2). In Harris *et al*'s model this is the overwhelmingly
318 principal species for In. On the other hand, the model of Biver *et al*., which complete
319 disregards the species $InH(NTA)_2$, agrees much better with AGNES results in the
320 probed conditions, albeit for the highest probed NTA concentration when Biver *et al*'s
321 predictions is somewhat higher than the free concentration measured by AGNES. In

summary, AGNES confirms the accuracy of Biver's constants in concentration regions where the discrepancies in predicted [In^{3+}] span several orders of magnitude.

3.3.2 In+Oxalate

A second speciation experiment involved a ligand (oxalate) which had been seen to form labile complexes with Zn (Companys et al., 2005). A titration of a fixed amount of In with increasing amounts of oxalate is shown in Fig. 6. The green dashed line shows the expected concentration according to VMINTEQ 3.1 using its standard database, where the In-Oxalate constants are taken from NIST 46.6 (which, in turn, takes the stability constant values from Pingarron and coworkers (Pingarron et al., 1984)). The thermodynamic accumulative stability constants derived from the NIST values (i.e. extrapolating at zero ionic strength) are log β^0_{110}=7.3; log β^0_{120}=13.19; log β^0_{130}=15.82; log β^0_{111}=8.16 (where the subscripts indicate the metal, ligand and proton stoichiometry, respectively). AGNES results diverge from this standard prediction, with values very close to the predictions based on the constants more recently reported by (Vasca et al., 2003): log β^0_{110}=7.95; log β^0_{120}=13.57; log β^0_{130}=15.5 (with the complex $InOxH^{2+}$ not being specifically considered). Notice the good agreement between AGNES and Vasca *et al*.'s prediction over five orders of magnitude variation in the free In concentration (almost from millimolar to nanomolar). Due to the decreasing [In^{3+}] at each oxalate addition, the gain had to be increased (see label close to each point in the figure). However, the deposition time (t_1-t_w) could be kept to just 25 s and reached equilibrium (checked with longer times). This is not contradictory with the time rule (11), because, in this case, the complexes of In with oxalates contribute to the flux (Companys et al., 2005). These complexes must be very labile and mobile (i.e. diffusion coefficient similar to that of the free ion), because their contribution to the arrival of In^{3+} at the electrode surface is so large.

4. Conclusions

The determination of free In^{3+} concentration at pH 3 using the electroanalytical technique AGNES has been successfully achieved. The partial irreversibility of indium leads to inaccuracies in the computation of the gain from DPP peaks (as was the case for Zn and Cd at very low ionic strengths (Aguilar et al., 2013b)), but they can be overcome by means of a new calibration strategy where the gain (rather than η_Q) is the calibrated parameter (see eqns. (4), (7) and (9)). The times required to attain equilibrium are slightly longer than the ones needed for reversible metals like Pb, Cd, and Zn, following the rule indicated in eqn. (11) rather than in eqn. (10).

Speciation of indium at pH 3 in systems containing either inert (with NTA) or labile (with oxalate) complexes can be followed with AGNES which discriminates between different published set of constants (models). Values reported in NIST 46.6 seems to be less accurate than other more recently published ((Biver et al., 2008) for In-NTA and (Vasca et al., 2003) for In-oxalate).

Very promising appears to be the application of AGNES in the presence of labile complexes, like In-oxalate complexes, where very short deposition times are enough, even for very low free concentrations, due to the contribution of the complexes to attain the equilibrium. Further work is needed to evaluate the effect of pH on In speciation and measurement. Current assessments of the stability constants -for oxalate or NTA- at pH 3 do not rely on any particular set of In hydrolysis (contrarily to what happens in other methods such as the potentiometric titrations (Biver et al., 2008)).

The application of AGNES to uncontaminated circumneutral natural waters still requires further challenging developments, such as the use of very small mercury electrodes combined with vigorous stirring to substantially decrease the diffusion layer (Rocha et al., 2010). Application to acid waters of streams impacted by mines seems, in principle, feasible with some adaptations of the existing methodology.

373

374 Acknowledgments

375 The authors gratefully acknowledge support for this research from the Spanish Ministry
376 MINECO (Projects CTM2013-48967 and CTM2016-78798-C2-1-P). MHT
377 acknowledges the Generalitat of Catalonia for a Ph.D. grant (FI AGAUR).

378

References

Abbas MN, Amer HS. A Solid-Contact Indium(III) Sensor based on a Thiosulfinate Ionophore Derived from Omeprazole. Bulletin of the Korean Chemical Society 2013; 34: 1153-1159.

Adam N, Schmitt C, Galceran J, Companys E, Vakourov A, Wallace R, Knapen D, Blust R. The chronic toxicity of ZnO nanoparticles and ZnCl2 to Daphnia magna and the use of different methods to assess nanoparticle aggregation and dissolution. Nanotoxicology 2014; 8: 709-717.

Aguilar D, Galceran J, Companys E, Puy J, Parat C, Authier L, Potin-Gautier M. Non-purged voltammetry explored with AGNES. Phys Chem Chem Phys 2013a; 15: 17510-17521.

Aguilar D, Parat C, Galceran J, Companys E, Puy J, Authier L, Potin-Gautier M. Determination of free metal ion concentrations with AGNES in low ionic strength media. J Electroanal Chem 2013b; 689: 276-283.

Alberti G, Biesuz R, Huidobro C, Companys E, Puy J, Galceran J. A comparison between the determination of free Pb(II) by two techniques: Absence of Gradients and Nernstian Equilibrium Stripping and Resin Titration. Anal Chim Acta 2007; 599: 41-50.

Alekseev VG, Myasnikova EN, Nikol'skii VM. Hydrolysis constants of Al3+, Ga3+, and In3+ ions in 0.1 M KNO3 solution. Russian Journal of Inorganic Chemistry 2013; 58: 1593-1596.

Alibo DS, Amakawa H, Nozaki Y. Determination of indium in natural waters by flow injection inductively coupled plasma mass spectrometry. Proceedings of the Indian Academy of Sciences-Earth and Planetary Sciences 1998; 107: 359-366.

Almagro V, Pena MJ, Sancho J. Polarographic Study on Reduction of In(Iii). Anales De Quimica 1977; 73: 1409-1414.

Bard AJ, Faulkner LR. Electrochemical Methods. Fundamentals and Applications. John Wiley & Sons, Inc., New York, 2001, 1-833 pp.

Biver T, Friani R, Gattai C, Secco F, Tine MR, Venturini M. Mechanism of indium(III) exchange between NTA and transferrin: A kinetic approach. J Phys Chem B 2008; 112: 12168-12173.

Charalambous A, Economou A. A study on the utility of bismuth-film electrodes for the determination of In(III) in the presence of Pb(II) and Cd(II) by square wave anodic stripping voltammetry. Anal Chim Acta 2005; 547: 53-58.

Chito D, Weng L, Galceran J, Companys E, Puy J, van Riemsdijk WH, van Leeuwen HP. Determination of free Zn^{2+} concentration in synthetic and natural samples with AGNES (Absence of Gradients and Nernstian Equilibrium Stripping) and DMT (Donnan Membrane Technique). Sci Total Envir 2012; 421-422: 238-244.

Chung YH, Lee CW. Electrochemical behaviors of Indium. Journal of Electrochemical Science and Technology 2012; 3: 1-13.

Companys E, Cecília J, Codina G, Puy J, Galceran J. Determination of the concentration of free Zn^{2+} with AGNES using different strategies to reduce the deposition time. J Electroanal Chem 2005; 576: 21-32.

Companys E, Puy J, Galceran J. Humic acid complexation to Zn and Cd determined with the new electroanalytical technique AGNES. Environ Chem 2007; 4: 347-354.

David C, Galceran J, Rey-Castro C, Puy J, Companys E, Salvador J, Monné J, Wallace R, Vakourov A. Dissolution kinetics and solubility of ZnO nanoparticles followed by AGNES. J Phys Chem C 2012; 116: 11758-11767.

Diaz-de-Alba M, Galindo-Riano MD, Pinheiro JP. Lead electrochemical speciation analysis in seawater media by using AGNES and SSCP techniques. Environ Chem 2014; 11: 137-149.

Domingos RF, Carreira S, Galceran J, Salaün P, Pinheiro JP. AGNES at vibrated gold microwire electrode for the direct quantification of free copper concentrations. Anal Chim Acta 2016; 920: 29-36.

Domingos RF, Huidobro C, Companys E, Galceran J, Puy J, Pinheiro JP. Comparison of AGNES (Absence of Gradients and Nernstian Equilibrium Stripping) and SSCP (Scanned Stripping Chronopotenciometry) for Trace Metal Speciation Analysis. J Electroanal Chem 2008; 617: 141-148.

Domingos RF, Simon DF, Hauser C, Wilkinson KJ. Bioaccumulation and Effects of CdTe/CdS Quantum Dots on Chlamydomonas reinhardtii - Nanoparticles or the Free Ions? Environ Sci Technol 2011; 45: 7664-7669.

Engblom SO, Ivaska AU. Characteristic Criteria for A Reversible-Reaction in Ac Polarography. J Electroanal Chem 1987; 222: 11-20.

Esteban M, Ruisanchez I, Larrechi MS, Rius FX. Expert system for the voltammetric determination of trace-metals .1. Determination of copper, zinc, cadmium, lead and indium. Anal Chim Acta 1992; 268: 95-105.

Galceran J, Chito D, Martinez-Micaelo N, Companys E, David C, Puy J. The impact of high Zn^{o} concentrations on the application of AGNES to determine free Zn(II) concentration. J Electroanal Chem 2010; 638: 131-142.

Galceran J, Companys E, Puy J, Cecília J, Garcés JL. AGNES: a new electroanalytical technique for measuring free metal ion concentration. J Electroanal Chem 2004; 566: 95-109.

Galceran J, Huidobro C, Companys E, Alberti G. AGNES: a technique for determining the concentration of free metal ions. The case of Zn(II) in coastal Mediterranean seawater. Talanta 2007; 71: 1795-1803.

Galceran J, Lao M, David C, Companys E, Rey-Castro C, Salvador J, Puy J. The impact of electrodic adsorption on Zn, Cd or Pb speciation measurements with AGNES. J Electroanal Chem 2014; 722-723: 110-118.

Galus Z. Diffusion-Coefficients of Metals in Mercury. Pure Appl Chem 1984; 56: 635-644.

Gupta VK, Hamdan AJ, Pal MK. Comparative study on 2-amino-1,4-naphthoquinone derived ligands as indium (III) selective PVC-based sensors. Talanta 2010; 82: 44-50.

Guru AK, Mahajan AV. Polarographic Studies of Indium (Iii) Complex with Sodium Oxalate. Current Science 1976; 45: 492-494.

Gustafsson, J. P. Visual MINTEQ version 3.1. https://vminteq.lwr.kth.se/download/. 2016.

Harris WR, Chen Y, Wein K. Equilibrium-Constants for the Binding of Indium(Iii) to Human Serum Transferrin. Inorg Chem 1994; 33: 4991-4998.

Huidobro C, Companys E, Puy J, Galceran J, Pinheiro JP. The use of microelectrodes with AGNES. J Electroanal Chem 2007; 606: 134-140.

Kariuki S, Dewald HD. Polarographic determination of diffusion coefficient values of In(III) in potassium chloride and nitrate supporting electrolytes. Talanta 1997; 44: 1765-1771.

Komatsu M. Potential-Step Anodic Stripping Voltammetry. Bull Chem Soc Jpn 1973; 46: 1670-1674.

Mu QS, David CA, Galceran J, Rey-Castro C, Krzeminski L, Wallace R, Bamiduro F, Milne SJ, Hondow NS, Brydson R, Vizcay-Barrena G, Routledge MN, Jeuken LJC, Brown AP. Systematic Investigation of the Physicochemical Factors That Contribute to the Toxicity of ZnO Nanoparticles. Chem Res Toxicol 2014; 27: 558-567.

Nosal-Wiercinska A. Catalytic activity of thiourea and its selected derivatives on electroreduction of In(III) in chlorates(VII). Central European Journal of Chemistry 2010; 8: 1-11.

Paquin PR, Gorsuch JW, Apte S, Batley GE, Bowles KC, Campbell PGC, Delos CG, Di Toro DM, Dwyer RL, Galvez F, Gensemer RW, Goss GG, Hogstrand C, Janssen CR, McGeer JC, Naddy RB, Playle RC, Santore RC, Schneider U, Stubblefield WA, Wood CM, Wu KB. The biotic ligand model: a historical overview. Comp Biochem Physiol C 2002; 133: 3-35.

Parat C, Authier L, Aguilar D, Companys E, Puy J, Galceran J, Potin-Gautier M. Direct determination of free metal concentration by implementing stripping chronopotentiometry as second stage of AGNES. Analyst 2011; 136: 4337-4343.

Parat C, Authier L, Castetbon A, Aguilar D, Companys E, Puy J, Galceran J, Potin-Gautier M. Free Zn2+ determination in natural freshwaters of the Pyrenees: towards on-site measurements with AGNES. Environ Chem 2015; 12: 329-337.

Pearson HBC, Galceran J, Companys E, Braungardt C, Worsfold P, Puy J, Comber S. Absence of Gradients and Nernstian Equilibrium Stripping (AGNES) for the determination of [Zn2+] in estuarine waters. Anal Chim Acta 2016; 912: 32-40.

496 Perez-Rafols C, Serrano N, Diaz-Cruz JM, Arino C, Esteban M. Simultaneous
497 determination of Tl(I) and In(III) using a voltammetric sensor array . Sensor Actuator B
498 Chem 2017; 245: 18-24.

499 Pingarron JM, Gallego-Andreu R, Sanchez-Batanero P. Potentiometric determination of
500 stability constants of complexes formed by indium(III) and different chelating agents.
501 Bulletin de la Societe Chimique de France 1984; 3-4: 115-122.

502 Puy J, Galceran J, Huidobro C, Companys E, Samper N, Garcés JL, Mas F. Conditional
503 Affinity Spectra of Pb^{2+}-Humic Acid Complexation from Data Obtained with AGNES.
504 Environ Sci Technol 2008; 42: 9289-9295.

505 Rocha LS, Companys E, Galceran J, Carapuca HM, Pinheiro JP. Evaluation of thin
506 mercury film rotating disc electrode to perform Absence of Gradients and Nernstian
507 Equilibrium Stripping (AGNES) measurements. Talanta 2010; 80: 1881-1887.

508 Rocha LS, Galceran J, Puy J, Pinheiro JP. Determination of the Free Metal Ion
509 Concentration Using AGNES Implemented with Environmentally Friendly Bismuth
510 Film Electrodes. Anal Chem 2015; 87: 6071-6078.

511 Rotureau E. Analysis of metal speciation dynamics in clay minerals dispersion by
512 stripping chronopotentiometry techniques. Colloids Surf A 2014; 441: 291-297.

513 Statsyuk VN, Dergacheva MB. Change in pHs of near-electrode layer of the dropping
514 mercury electrode in the course of electrolytic reduction of molecular oxygen in
515 polarographic determination of Indium(III), Cadmium(II) and Thallium(I). Russ J Gen
516 Chem 1998; 68: 691-693.

517 Taher MA. Differential pulse polarography determination of indium after column
518 preconcentration with [1-(2-pyridylazo)-2-naphthol]-naphthalene adsorbent or its
519 complex on microcrystalline naphthalene. Talanta 2000; 52: 301-309.

520 Tuck DG. Critical Survey of Stability-Constants of Complexes of Indium. Pure Appl
521 Chem 1983; 55: 1477-1528.

522 Turnham DS. 2. Polarographic Diffusion Coefficients of Some Simple Cations in
523 Various Electrolytes Calculated for Infinite Dilution and Under Polarographic
524 Conditions. J Electroanal Chem 1965; 10: 19-&.

525 Vale G, Franco C, Brunnert AM, dos Santos MMC. Adsorption of Cadmium on
526 Titanium Dioxide Nanoparticles in Freshwater Conditions - A Chemodynamic Study.
527 Electroanal 2015; 27: 2439-2447.

528 Vasca E, Ferri D, Manfredi C, Torello L, Fontanella C, Caruso T, Orru S. Complex
529 formation equilibria in the binary Zn2+-oxalate and In3+-oxalate systems. Dalton Trans
530 2003; 2698-2703.

531 White SJO, Hemond HF. The Anthrobiogeochemical Cycle of Indium: A Review of the
532 Natural and Anthropogenic Cycling of Indium in the Environment. Critical Reviews in
533 Environmental Science and Technology 2012; 42: 155-186.

White SJO, Hussain FA, Hemond HF, Sacco SA, Shine JP, Runkel RL, Walton-Day K, Kimball BA. The precipitation of indium at elevated pH in a stream influenced by acid mine drainage. Sci Total Envir 2017; 574: 1484-1491.

Wood SA, Samson IM. The aqueous geochemistry of gallium, germanium, indium and scandium. Ore Geology Reviews 2006; 28: 57-102.

Zavarise F, Companys E, Galceran J, Alberti G, Profumo A. Application of the new electroanalytical technique AGNES for the determination of free Zn concentration in river water. Anal Bioanal Chem 2010; 397: 389-394.

Zelic M, Mlakar M, Branica M. Influence of Perchlorates and Halides on the Electrochemical Properties of Indium(Iii). Anal Chim Acta 1994; 289: 299-306.

Zhang LM, Li JP, Zeng Y, Meng LH, Fu C. Highly Selective Molecularly Imprinted Polymer Sensor for Indium Detection Based on Recognition of In-Alizarin Complexes. Electroanal 2015; 27: 1758-1765.

Zimmermann YS, Schaffer A, Corvini PFX, Lenz M. Thin-Film Photovoltaic Cells: Long-Term Metal(loid) Leaching at Their End-of-Life. Environmental Science & Technology 2013; 47: 13151-13159.

552
553
554 Table 1 Composition of the mixtures NTA+In and AGNES parameters applied at pH 3.00±0.03 ($t_{1,a}$=0 indicates a 1P strategy) with KNO_3 0.1
555 mol L^{-1} as supporting electrolyte.
556
557
558

pH	$c_{T,In}$ / μmol L^{-1}	$c_{T,NTA}$ / μmol L^{-1}	$[In^{3+}]$ AGNES / μmol L^{-1}	$[In^{3+}]$ VMINTEQ / μmol L^{-1}	$t_{1,a}$ / s	*Y*	t_1-t_w or $t_{1,b}$ / s	% $[In^{3+}]$ VMINTEQ
3.001	9.88	0.00	9.84	8.17	0	10, 20	200, 400	82.7
2.998	10.31	0.00	8.40	8.54	0	2, 5	100, 200	82.5
2.992	10.34	0.00	8.84	8.51	0	2, 5	100, 200	82.6
3.033	9.87	2.37	6.79	8.53	0	2,10,20	100, 200, 400	62.9
3.015	10.30	4.86	4.51	6.21	0	5, 10	200, 400	44.1
3.003	10.33	4.87	5.14	4.54	0	5, 10	200, 400	44.1
2.997	10.33	4.87	5.14	4.56	0	5, 10	100, 200	44.1
3.013	9.87	5.11	4.03	4.56	0	5,10	200, 400	40.5
3.014	10.29	7.77	2.01	3.99	0	10, 20	200, 400	21.9
2.999	10.32	7.79	2.11	2.26	0	10, 20	200, 400	22.0
3.005	10.32	7.79	2.18	2.27	0	10, 20	200, 400	22.0
2.997	10.31	9.44	0.632	2.27	0	15, 30	200, 400, 800	0.021
3.007	10.26	9.44	1.05	1.14	0	20, 50	200, 400, 800 (for *Y*=20) 500, 1000, 2000 (for *Y*=50)	11.1
3.015	10.30	12.24	1.93×10^{-3}	1.11	1.5, 5	10000	5000, 10000	2.72

3.000	10.20	12.82	1.20×10^{-3}	0.280	6, 10, 12, 20	1×10^{4}, 2×10^{4}	2000	2.23
3.004	8.56	14.78	1.72×10^{-4}	0.227	8, 10, 9	5×10^{4}, 5×10^{3}	1000, 2000	1.03
3.004	8.59	14.84	1.58×10^{-4}	0.0880	18, 9	1×10^{5}, 5×10^{4}	1000, 2000	1.02

572
573 Table 2 Logarithm of the accumulated thermodynamic stability constants
574 (β^0 or β^{th}) for In+NTA complexes from the literature.

	log β^{th}		
Complex formed	Default VMINTEQ database	Harris *et al.* (Harris et al., 1994)	Biver *et al.* (Biver et al., 2008)
In NTA	15.73	15.74	18.39
In $(NTA)_2$	25.62	25.63	27.99
$InH(NTA)_2$	18.6	29.14	-

575
576

577

578 # Figures

579

580

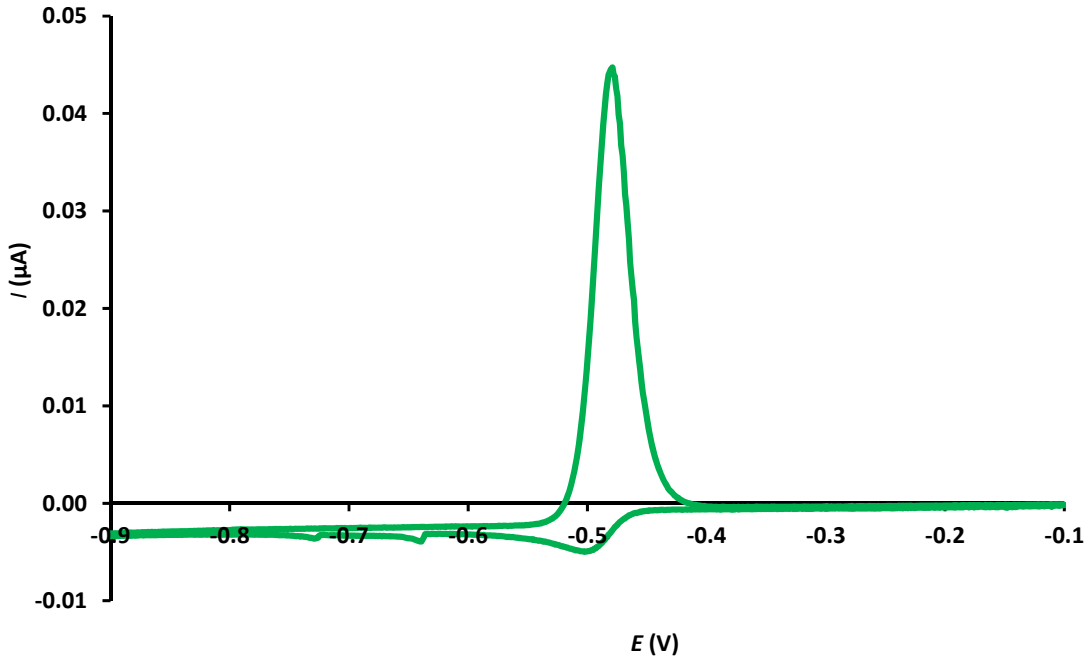

581

582 *Fig 1: Cyclic voltammogram in* $c_{T,In}$*=4.98µmol* L^{-1} *at pH=3 between -0.1V and --0.9V,*
583 *scan rate 10 mV/s. Measured:* E_c *= -0.502 V,* E_a *= - 0.479 V. The distance between the*
584 *peaks is 23 mV.*

585

586

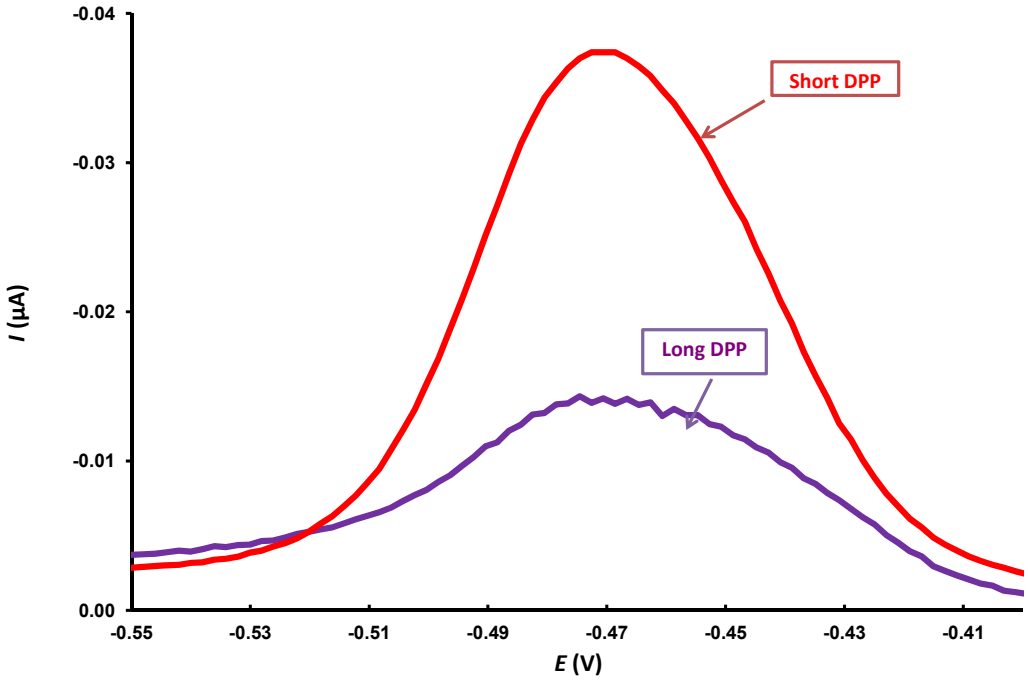

587

588 *Fig 2: Differential Pulse Polarograms in an indium solution 4.90 µmol L^{-1} at pH=3.*
589 *Purple line stands for the "long" or "standard" DPP (t_d=1s) while the red line stands*
590 *for the "short" DPP (t_d=0.1s).*
591

592

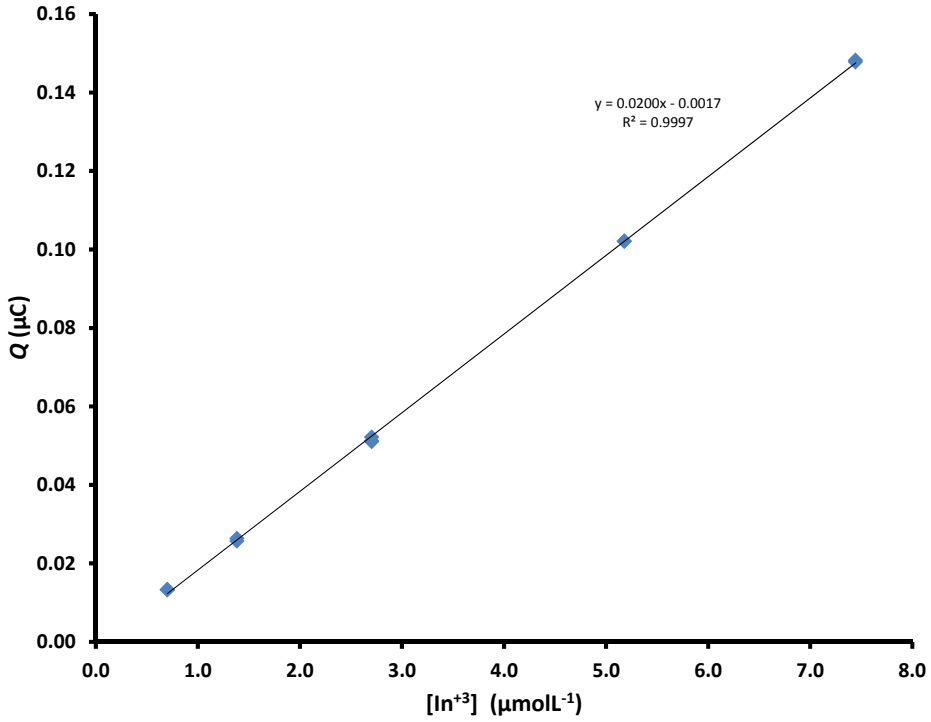

Fig 3: Calibration of In for faradaic charges (Q) at pH=3 using E_{calib}=-0.4996 V. From the slope, Y_{calib}=5.90 was derived. The free indium concentration in abscissae is computed with the speciation program VisualMinteq.

a)

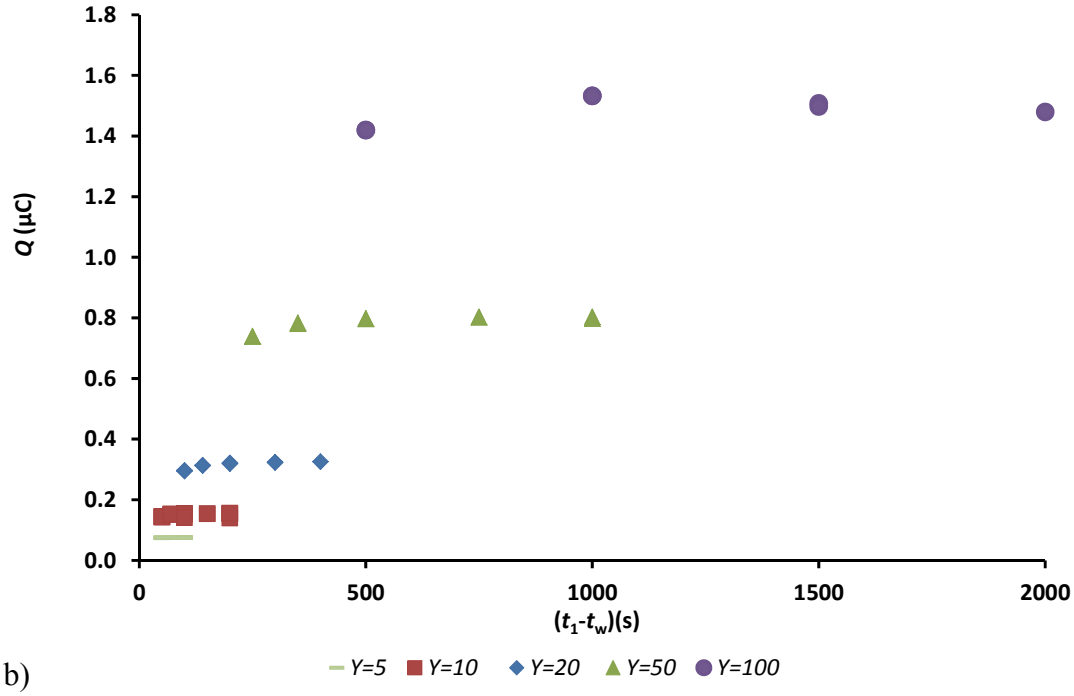

b)

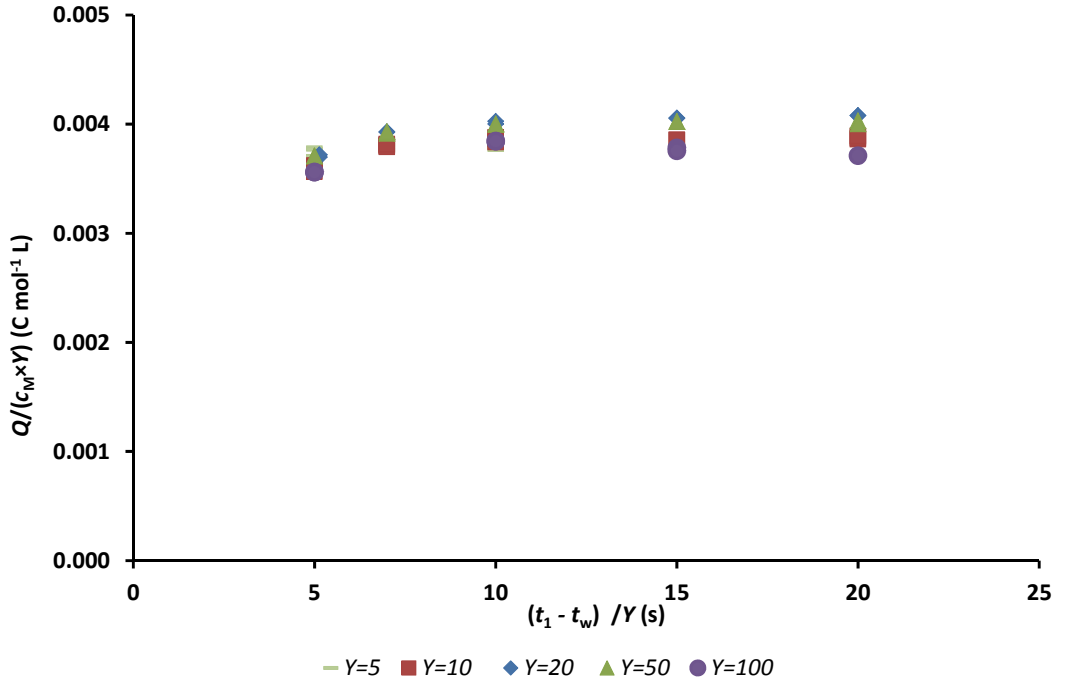

Fig 4: Trajectories at different gains in a solution $c_{T,In}$=5.00 µmol L^{-1} at pH=3. Panel a) Charge vs. deposition time with stirring; Panel b) Collapse of the trajectories using normalized charge vs. normalized time.

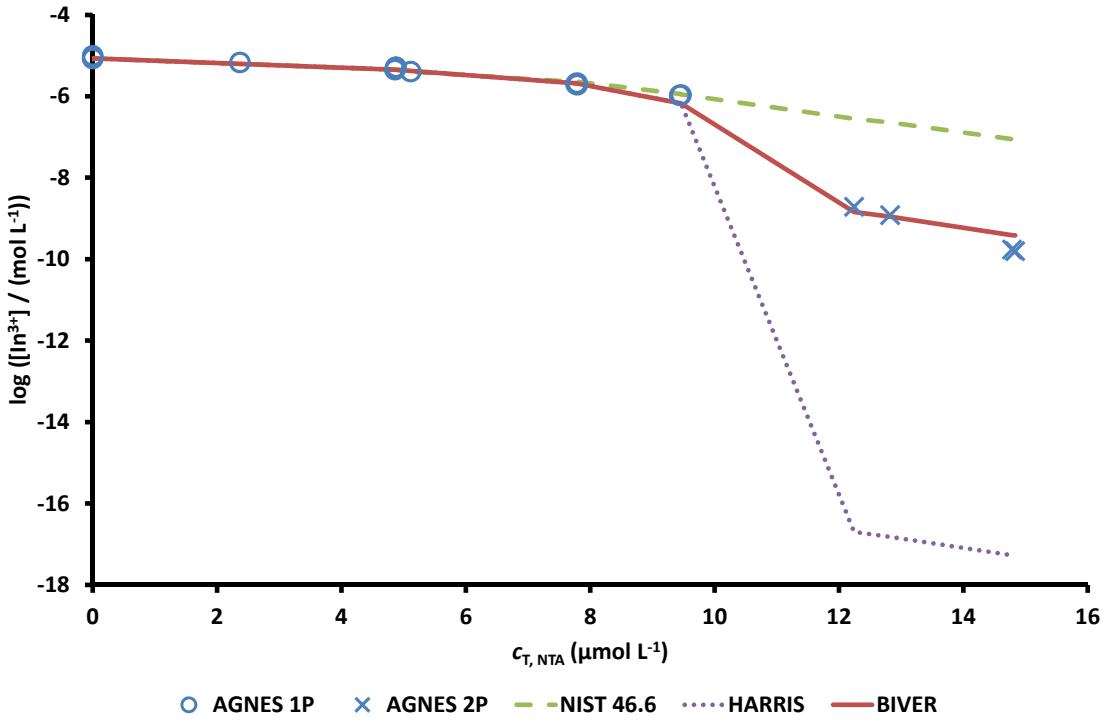

608

609 *Fig 5: Free indium concentrations for several mixtures of In ($c_{T,In}$ around 10 µmol L-*
610 *1) with NTA at pH=3 (see table 1). Circle markers stand for AGNES 1 pulse*
611 *measurements, while cross markers stand for AGNES 2 pulses measurements.*
612 *Theoretical computations using VMINTEQ: Green dashed line for database NIST 46.6*
613 *(default in VMINTEQ); violet dotted line for values from Harris et al (1994), and*
614 *continuous red line for values from (Biver et al (2008) .*
615

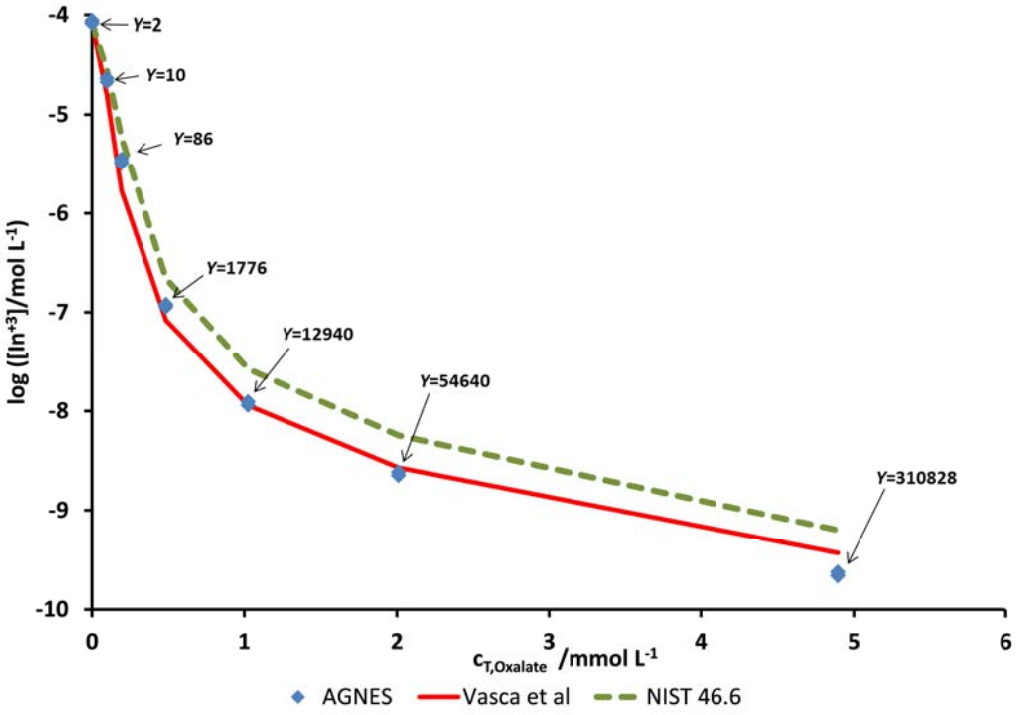

Fig 6: Free indium concentrations along a titration of an initial indium concentration 5 µmol L^{-1} with increasing amounts of oxalate at pH 3. Dashed green line: theoretical expectation according to stability constants in NIST 46.6; Continuous red line: theoretical expectations according to the stability constants of Vasca et al. (2003). Diamond markers: experimental results obtained with AGNES. Gains are indicated with labels. Deposition time, t_1-t_w, 25 s.

SUPPLEMENTARY MATERIAL

Free Indium concentration determined with AGNES

Marjan H. Tehrani, Encarna Companys*, Angela Dago, Jaume Puy and Josep Galceran

Departament de Química. Universitat de Lleida, and AGROTECNIO, Rovira Roure 191, 25198 Lleida, Catalonia, Spain

* corresponding author ecompanys@quimica.udl.cat

in Science of the Total Environment (2017)

TABLE OF CONTENTS:

1. Composition of calibration solutions

Table 1: Computed free In concentrations and percentages of the other main species in the solutions used for the calibration shown in Fig. 3 of the article.

Table SM-1: Specifications of calibration solutions

Code	$c_{T,In}$ (µmol L^{-1})	pH	$[In^{3+}]_{VMINTEQ}$ (µmol L^{-1})	$\%In^{3+}$	$\%InNO_3^{2+}$	$\%In(OH)_2^{+}$	$\%InOH^{2+}$
M_1	0.85	2.997	0.70	82.5	14.4	0.18	2.86
M_2	1.67	3.002	1.38	82.6	14.3	0.19	2.91
M_3	3.26	3.000	2.70	82.7	14.1	0.19	2.93
M_4	6.24	3.002	5.18	83.0	13.8	0.20	3.00
M_5	8.94	3.002	7.44	83.2	13.5	0.20	3.06

2. Ancillary electroanalytical techniques

This section expands the ancillary electroanalytical techniques that have been used in the article: DPP (Differential pulse polarography) and CV (Cyclic voltammetry). It briefly introduces each technique and explain its principles. The purpose is to provide an overview of each technique and point out their potentials and limitations.

2.1 DPP (Differential pulse polarography)

Differential pulse polarography is a polarographic technique (i.e. based on the use of a mercury drop as working electrode) whose potential program is a series of separated potential steps (Arca et al., 1995;Bard and Faulkner, 1980). Fig. SM-1 shows that the potential program is a combination of a linear ramp with a superimposed square wave. During each drop, two potentials are applied: the base potential E_b during a time denoted t_0 (first pulse) and the potential $E_b + \Delta E$ during a time $t_p = t_d - t_0$ (second pulse or

pulse width). The polarogram takes, for each drop, the base potential as abscissa while, for ordinate, it takes the difference between two current samples: one immediately before the time t_0 and the other just before the end of the drop lifetime (t_d).

In uncomplicated systems (i.e. just metal ions and background electrolyte with negligible complexation), the height of the peak is proportional to the free metal ion concentration (which is also the total metal concentration), but such proportionality vanishes -in general- when the metal is complexed. Relatively cumbersome mathematical expressions are needed to describe the differential pulse polarogram, even in cases without electrodic adsorption.

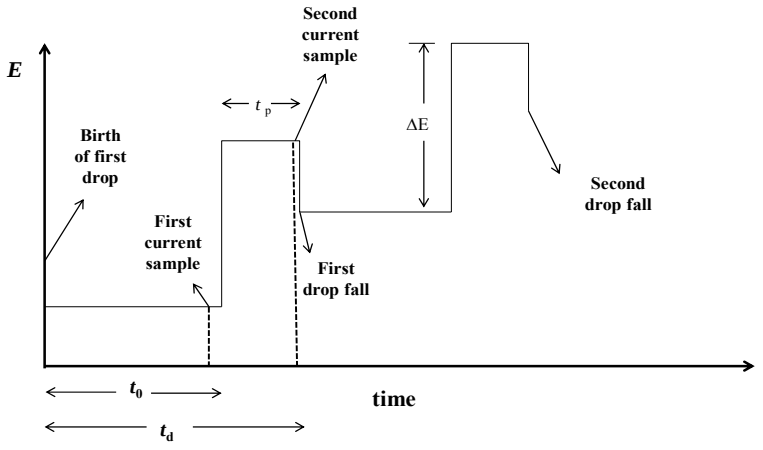

Fig SM-1: Potential program for two drops in a differential pulse polarographic experiment. Adapted from reference (Bard and Faulkner, 1980).

Assuming a reversible redox couple and planar electrode, the peak potential (E_{peak}) or position of the maximum of the polarogram can be computed (see eqn. (7.3.30) in reference (Bard and Faulkner, 1980)) with

$$E_{peak} = E^{0'} + \frac{RT}{nF} \ln \sqrt{\frac{D_{M^0}}{D_{M^{n+}}}} - \frac{\Delta E}{2} \quad \text{(SM.1)}$$

where $E^{o'}$ is the standard formal potential of the redox couple, R is the gas constant, T is the temperature, n is the number of exchanged electrons, F is the Faraday constant, D_{M^0} is the diffusion coefficient for the reduced metal inside the amalgam, $D_{M^{n+}}$ is the diffusion coefficient for the free metal ion in solution and ΔE is the modulation amplitude (or pulse height).

DPP is an ancillary technique for AGNES because the gain can be computed from E_{peak} for several analytes (Zn, Cd, Pb, Sn). See eqn. 5 in the manuscript.

Complexation of the electroactive metal (with ligands including OH^-) changes the position of the DPP peak and its height. So, in the particular case of indium, a low pH (such as 3) is convenient to avoid an impact on E_{peak} due to the formation of indium hydroxides.

2.2 CV (Cyclic Voltammetry)

Potential sweep methods are widely used to study electrode processes. One of the variants is Cyclic Voltammetry (CV), where the sweep direction is inverted at a certain chosen potential. The applied potential is varying within time in a symmetrical saw-tooth wave form (Brett and Oliveira-Brett, 1993) as shown in Fig

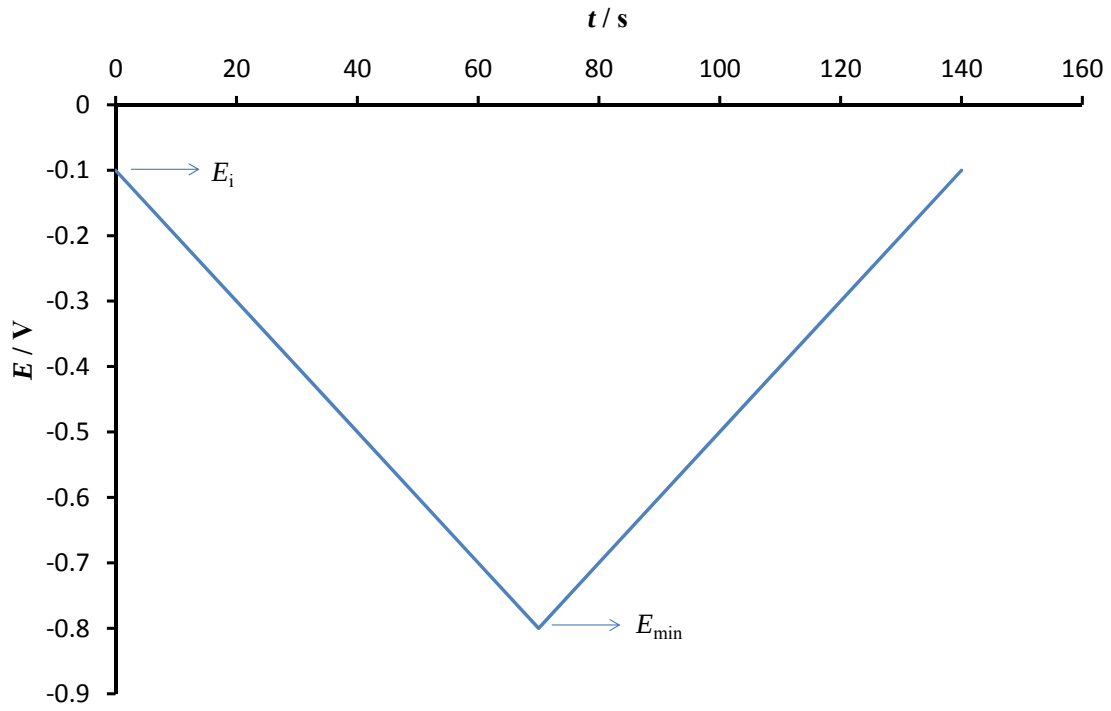

Fig SM-2:Variation of the applied potential with time in cyclic voltammetry, showing the initial potential, E_i = -0.1 V, and the return potential E_{min}= -0.8 V . *Adapted from reference (Brett and Oliveira-Brett, 1993).*

In this technique the resulting current is recorded over the whole cycle of forward and reverse sweeps. Species reduced in a forward scan of each cycle can be re oxidized in the reverse scan, hence in many simple systems two (cathodic and anodic) peaks appear which can be identified with the reduction and oxidation processes, respectively; see Fig SM-3.

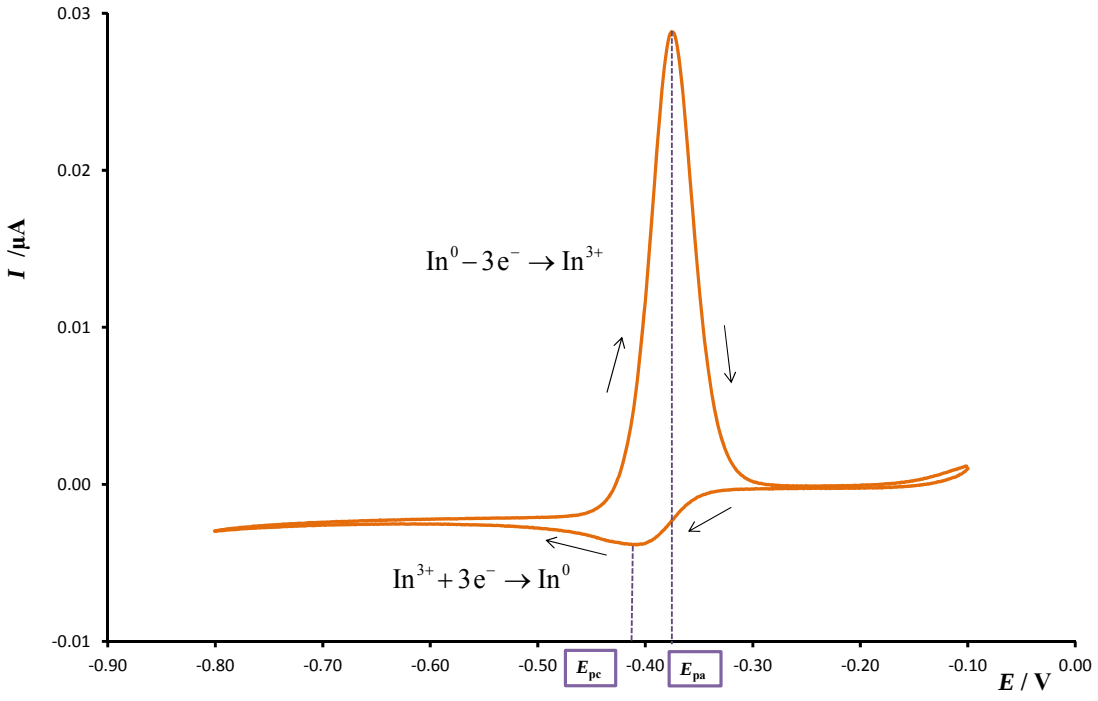

Fig SM-3: Schematic representation of the processes in the cyclic voltammogram applied to a solution with indium. $c_{T,In}$=0.10µmol L^{-1} at pH=3 between -0.1V and -0.8 V, scan rate 10 mV/s. Measured: E_c = -0.406 V, E_a = - 0.375 V. The distance between the peaks is 31 mV.

The electrode process is more irreversible if the separation between the peaks for forward and reverse scan is greater. As indicated in the article, at 25ºC, the difference between the anodic and cathodic peak potentials should be

$$\left|E_{pa} - E_{pc}\right| = \frac{RT}{nF}\ln(10) \approx \frac{59}{3}\,\text{mV} \approx 19\,\text{mV} \qquad (2)$$

for a fully reversible couple of a trivalent cation. In case of the fully irreversible system during the inversed scan direction no peak would appear (Brett and Oliveira-Brett, 1993).

CV is a typical technique in exploratory phases, to elucidate the main phenomena taking place at the electrode, but it is not very much used for quantitative purposes, due to the

cumbersome expressions that could be applicable (Bard and Faulkner, 1980;Crow, 1994) for its interpretation.

3. AGNES

3.1 Applications of AGNES

AGNES (Absence of Gradients Nernstian Equilibrium Stripping) has been successfully applied for determining free concentrations of metals in a wide range of systems such as natural samples (seawater (Galceran et al., 2007), river water (Chito et al., 2012;Zavarise et al., 2010), solutions containing dissolved organic matter (Companys et al., 2007;Pernet-Coudrier et al., 2011;Puy et al., 2008), soil extracts (Chito et al., 2012)).

AGNES has measured free metal ion concentrations of Zn, Cd and Pb (with HMDE or Screen Printed electrodes) (Galceran et al., 2014;Parat et al., 2011) and Cu (with solid electrodes) (Domingos et al., 2016).

3.2 Principles of AGNES

AGNES is a stripping technique consisting of two stages with specific goals. We detail here its principles when indium is the target analyte.

3.2.1 First stage: Absence of Gradients in the concentration profiles and Nernstian Equilibrium at the electrode surface

The aim of this stage is to reach a special situation of equilibrium, where two conditions have to be fulfilled: i) Absence of Gradients in the concentration profiles and ii) Nernstian equilibrium at the electrode surface.

Condition i) : Absence of Gradients. Fig Fig SM-4 shows a schematic representation of the desired concentration profiles. As can be seen on the left hand side (in the amalgam), there is a uniform concentration of reduced indium and, on the right hand, there is a flat concentration profile of free indium cation in the solution.

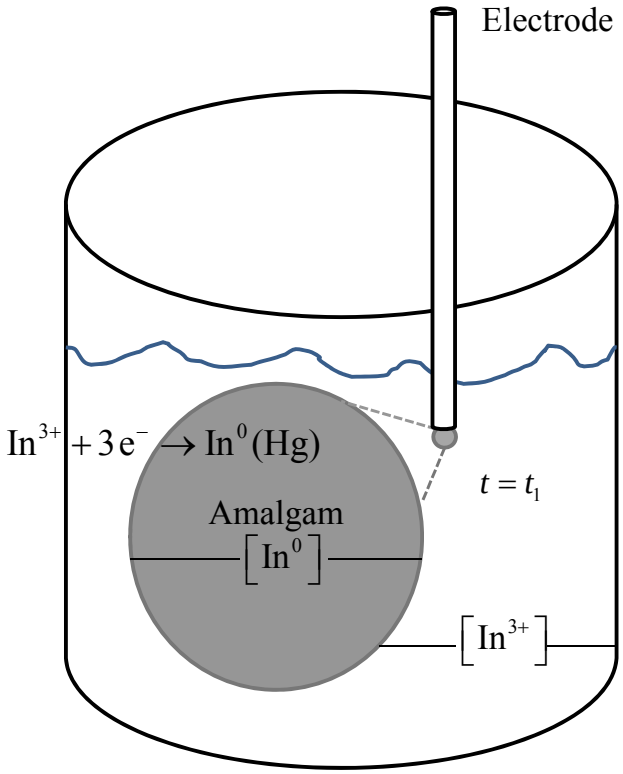

Fig SM-4: Profiles aimed at the end of the first step ($t=t_1$)

Condition ii): the second requirement is reaching Nernstian equilibrium for the redox couple (e.g. In^{3+}/In^0 in this work). The concentration of the oxidized and re-oxidized species of indium must fulfil Nernst equation which can be written as:

$$E = E^0 + \frac{RT}{3F} \ln \frac{a_{In^{3+}}}{a_{In^0}} \qquad \text{(SM.3)}$$

where E^0 is the standard redox potential and a_j is the activity of species j. When equilibrium is reached, Nernst equation can be re-written as

$$Y = \frac{\left[\mathrm{In}^{0}\right]}{\left[\mathrm{In}^{3+}\right]} = \exp\left[-\frac{3F}{RT}\left(E_1 - E^{0'}\right)\right] \quad \text{(SM.4)}$$

where Y is the gain or preconcentration factor, which represents the proportionality between the reduced indium concentration in the amalgam and its free form in the solution. E_1 is the deposition potential associated to the gain Y.

There are several ways to reach the two equilibrium conditions (i and ii). The simplest one is the 1P strategy, where the same potential E_1 is applied, while waiting for as long time (t_1) as needed to achieve the goal of the two equilibrium conditions. Fig SM-5 shows a scheme of the 1P strategy. Usually, the potential E_1 is just a few millivolts more negative than the standard redox potential of the couple, so that moderate gains are aimed, because larger gains require longer deposition times.

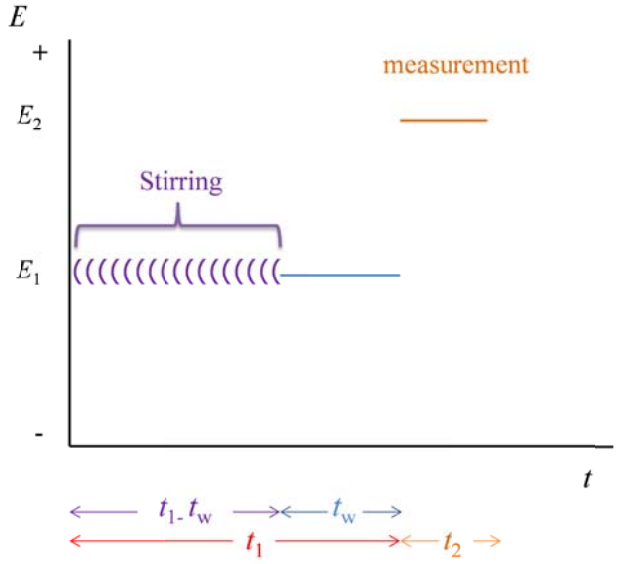

Fig SM-5: Representation of the simplest potential program (i.e. using one potential pulse, 1P) for the first stage. E_1 is the deposition potential associated to the concentration gain Y. In the variant AGNES-I, E_2 corresponds to a potential for a re-oxidation under diffusion limited conditions. t_w is the duration of the period of no stirring at the end of the deposition time.

Alternatively, especially for large *Y*, one may use the refined strategy "2 pulses" (or 2P). In this methodology, two potentials: $E_{1,a}$ and $E_{1,b}$ are applied in two sub-stages of the deposition stage, see Fig Fig SM-6. In the first sub-stage $E_{1,a}$ (prescribing diffusion limited conditions for deposition, which might be associated to a gain $Y_{1,a}$ which will never be attained) is applied during $t_{1,a}$. In the second sub-stage, the potential $E_{1,b}$ (corresponding to the desired gain *Y*) is applied during $t_{1,b}$ (which could be called "relaxation time").

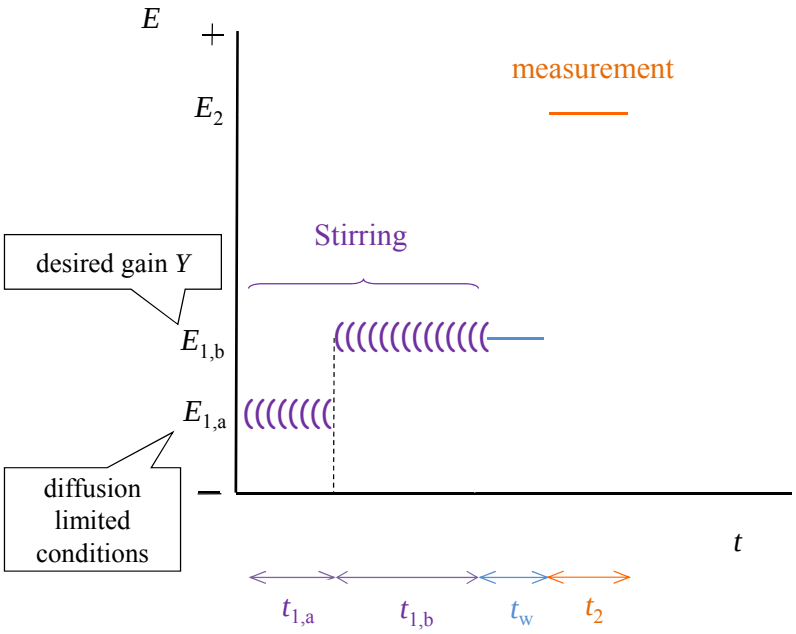

Fig SM-6: Schematic representation of the potential and stirring program using two potential sub-steps in the first stage (AGNES-2P). The total deposition time t_1 is the summation of the first potential step time $t_{1,a}$, the second potential $t_{1,b}$ and the waiting time t_w.

To enhance mass transport, stirring is activated along most of the deposition stage. See table SM-2 with the specification of the periods where stirring is on.

Table SM-2: Combination of parameters for the two strategies available for the first stage (1 Pulse and 2 Pulses) of AGNES .

a: Parameters for 1P

1 *P*	Stage	Time	Stirring	Potential	Gain
	Deposition	t_1-t_w	On	E_1	Y=Y_1
		t_w	Off	E_1	Y=Y_1
	Stripping	t_2	Off	E_2	Y_2

b: Parameters for 2P

2 *P*	Stage	Time	Stirring	Potential	Gain
	Deposition	$t_{1,a}$	On	$E_{1,a}$	$Y_{1,a}$
		$t_{1,b}$	On	E_1	Y=$Y_{1,b}$
		t_w	Off	E_1	Y=$Y_{1,b}$
	Stripping	t_2	Off	E_2	Y_2

After the application of the first sub-stage in 2P, three situations can arise: undershoot, equilibrium or overshoot. The undershoot appears when the number of moles accumulated during the first sub-stage (i.e. throughout the time $t_{1,a}$) is less than those needed for equilibrium. The overshoot appears when the number of moles is greater than those needed. Using the 2P strategy there is a reduction of the deposition time (with respect to the 1P strategy) that might even reach a factor of ten, if $t_{1,a}$ is optimally chosen. Fig SM-7 shows how a large overshoot can be spotted in the currents recorded during the first stage of a 2P experiment.

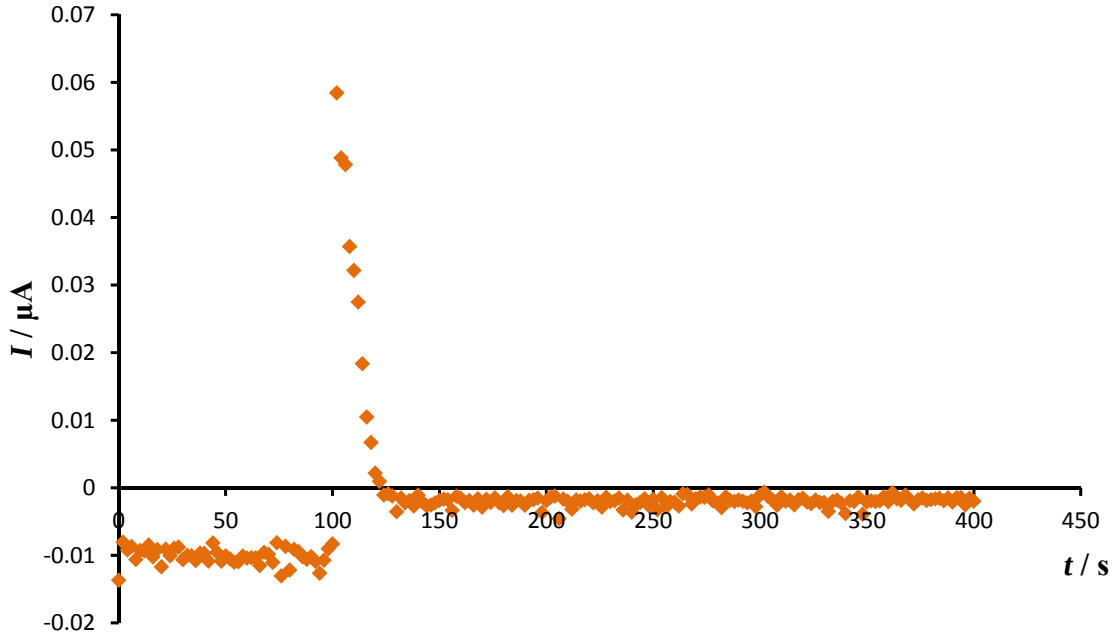

Fig SM-7: Currents recorded during the first stage of a 2P experiment. $Y_{1,a}=10^{10}$; Y=50; $t_{1,a}=100$ s; $t_{1,b}=300$ s; $c_{T,In}=4.97\mu mol\ L^{-1}$ and $c_{T,Ox}=69\mu mol\ L^{-1}$ and pH=3.00.

To check whether a given $t_{1,a}$ produces overshoot, undershoot or equilibrium in our system, one can compare experiments with various $t_{1,b}$. See Fig SM-8. If experiments with longer $t_{1,b}$ produce higher analytical responses (in the stripping stage), one concludes that the applied $t_{1,a}$ has been too short (i.e. undershoot). If longer $t_{1,b}$ produce lower analytical responses, one concludes that the applied $t_{1,a}$ has been too long (i.e. overshoot). Table SM-2 provides the times and potentials that were used for 1P and 2P.

Regardless of which strategy (1P or 2P) is adopted for the first stage, it is convenient to use small electrodes, as the required deposition time increases with the size of the electrode (Huidobro et al., 2007). So, drop size 1 -the smallest in our stand- is selected to reach to the equilibrium faster. Its approximate radius is 1.41×10^{-4}m.

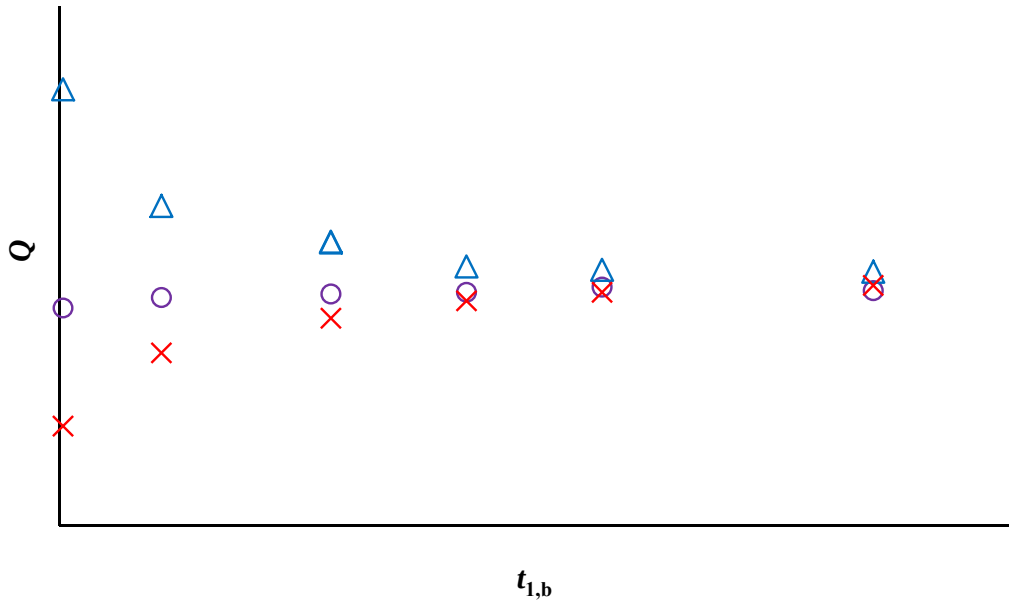

Fig SM-8: Schematic representation of possible situations for the first sub-stage of 2P experiments, as seen from the stripping charges (Q) in three series of experiments (each characterized by a given $t_{1,a}$) along increasingly long relaxation times ($t_{1,b}$). The markers triangle, circle and cross, represent overshoot, equilibrium and undershoot situations, respectively. The series indicated with triangle markers are associated to a $t_{1,a}$ larger than the optimum one (for the aimed gain), while the cross series are associated to too short $t_{1,a}$.

3.2.2 Second stage: quantification of the reduced indium inside the amalgam.

The goal of the second stage is to quantify how much In^0 has been accumulated in the amalgam during the first stage. There are different ways to achieve the goal of this second stage, which lead to the variants AGNES-I, AGNES-Q, AGNES-SCP and AGNELSV (Galceran et al., 2014).

In the case of indium, AGNES-Q has been selected, where the stripped charge is measured. Once discounted the blank (i.e. the capacitive charge in an experiment with

no analyte, just background electrolyte) (Galceran et al., 2014) from the total charge, one obtains the faradaic charge (Q). Acording to Faraday's law, one can write:

$$Q = 3F(\text{moles in amalgam}) = 3FV_{\text{Hg}}\left[\text{In}^{\text{o}}\right] \quad \text{(SM\_5)}$$

By defining the proportionality factor as

$$\eta_{\text{Q}} = 3FV_{\text{Hg}} \quad \text{(SM\_6)}$$

and combining with SM.4)

$$Q = \eta_{\text{Q}} Y[\text{In}^{3+}] \quad \text{(SM\_7)}$$

This expression indicates the direct proportionality between faradaic charge and the free concentration of indium in the solution.

During this second stage, it is necessary that all of the reduced indium inside the amalgam is stripped to have the total faradaic charge (Q). This total charge is not affected by any kinetics, provided the stripped charge is the one that corresponds to the total number of moles of In^0 in the amalgam. When all this In^0 is stripped, the speed at which this stripping is happening is irrelevant (as long as we wait long enough for the complete stripping).

During the second stage, the current is sampled at short time intervals (e.g. each 50 ms) and is is recorded into a file (see Fig SM-9). The integration of these currents provides the charge.

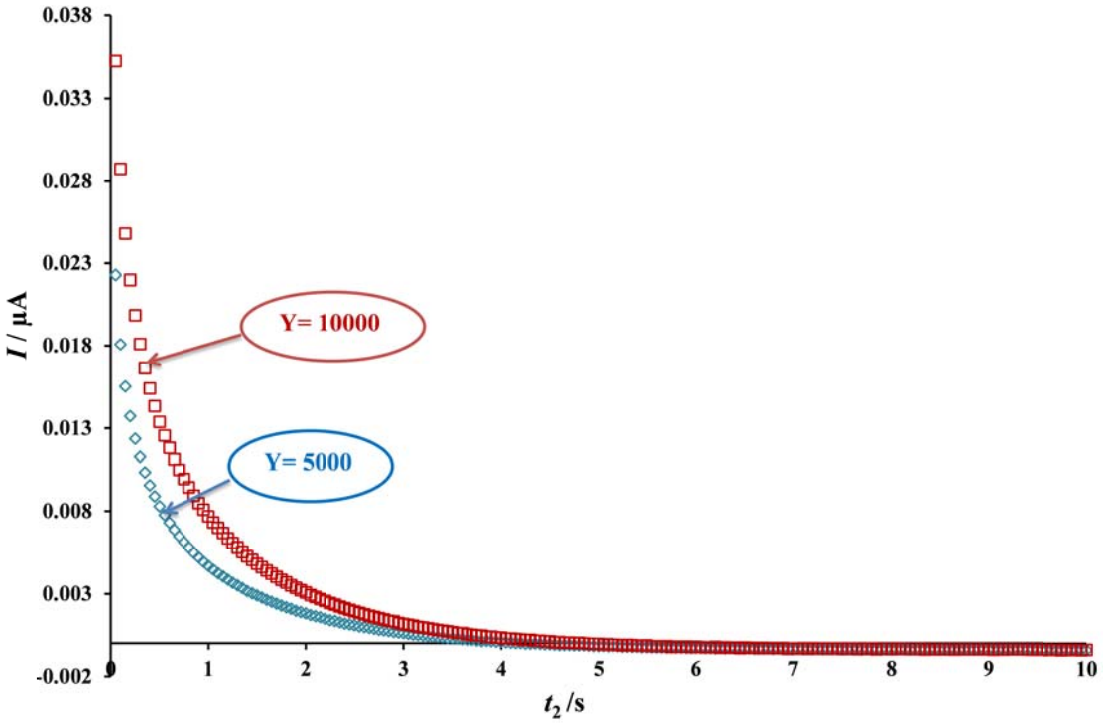

Fig SM-9: Stripping currents during the second stage. $c_{T,In}$ *=10.29 µmol* L^{-1} *and* $c_{T,NTA}$*=12.24µ mol* L^{-1}*,square marker represents the results using higher gain while the diamond marker stands for the results using lower gain.*

$$Q = \int_0^{t_2} I \, dt \qquad \text{(SM\_8)}$$

In practice, Q is just the summation of the cells (with faradaic intensity currents I_j) multiplied by the fixed interval time (Δt) in an Excel file (Galceran et al., 2010):

$$Q = \int_0^{t} I \, dt \approx \Delta t \left(\sum_{j=1}^{n_{max}} I_j \right) \qquad \text{(SM\_9)}$$

n_{max} is the number of intervals taken (usually 1000 intervals corresponding to the 50 s of t_2).

Complexation of the electroactive metal with ligands in the solution (including OH^-) does not impact on the equilibrium analytical response of AGNES, neither charge nor intensity, provided one is comparing solutions having the same free metal ion concentration. Moreover, the presence of ligands can only shorten the needed deposition

time, as they might contribute to the flux (if they are not totally inert) that builds up the required amount of reduced metal in the amalgam (Galceran et al., 2004).

References

Arca M, Mirkin MV, Bard AJ. Polymer-Films on Electrodes .26. Study of Ion-Transport and Electron-Transfer at Polypyrrole Films by Scanning Electrochemical Microscopy. J Phys Chem 1995; 99: 5040-5050.

Bard AJ, Faulkner LR. Electrochemical Methods, Fundamentals and Applications. Wiley, New York, 1980.

Brett CMA, Oliveira-Brett AM. Electrochemistry. Principles, methods and applications. Oxford University Press, Oxford (UK), 1993.

Chito D, Weng L, Galceran J, Companys E, Puy J, van Riemsdijk WH, van Leeuwen HP. Determination of free Zn^{2+} concentration in synthetic and natural samples with AGNES (Absence of Gradients and Nernstian Equilibrium Stripping) and DMT (Donnan Membrane Technique). Sci Total Envir 2012; 421-422: 238-244.

Companys E, Puy J, Galceran J. Humic acid complexation to Zn and Cd determined with the new electroanalytical technique AGNES. Environ Chem 2007; 4: 347-354.

Crow DR. Principles and applications of electrochemistry. Blackie Academic & Professional, London (UK), 1994.

Domingos RF, Carreira S, Galceran J, Salaün P, Pinheiro JP. AGNES at vibrated gold microwire electrode for the direct quantification of free copper concentrations. Anal Chim Acta 2016; 920: 29-36.

Galceran J, Chito D, Martinez-Micaelo N, Companys E, David C, Puy J. The impact of high Zn^{o} concentrations on the application of AGNES to determine free Zn(II) concentration. J Electroanal Chem 2010; 638: 131-142.

Galceran J, Companys E, Puy J, Cecília J, Garcés JL. AGNES: a new electroanalytical technique for measuring free metal ion concentration. J Electroanal Chem 2004; 566: 95-109.

Galceran J, Huidobro C, Companys E, Alberti G. AGNES: a technique for determining the concentration of free metal ions. The case of Zn(II) in coastal Mediterranean seawater. Talanta 2007; 71: 1795-1803.

Galceran J, Lao M, David C, Companys E, Rey-Castro C, Salvador J, Puy J. The impact of electrodic adsorption on Zn, Cd or Pb speciation measurements with AGNES. J Electroanal Chem 2014; 722-723: 110-118.

Huidobro C, Companys E, Puy J, Galceran J, Pinheiro JP. The use of microelectrodes with AGNES. J Electroanal Chem 2007; 606: 134-140.

Parat C, Authier L, Aguilar D, Companys E, Puy J, Galceran J, Potin-Gautier M. Direct determination of free metal concentration by implementing stripping chronopotentiometry as second stage of AGNES. Analyst 2011; 136: 4337-4343.

Pernet-Coudrier B, Companys E, Galceran J, Morey M, Mouchel JM, Puy J, Ruiz N, Varrault G. Pb-binding to various dissolved organic matter in urban aquatic systems: Key role of the most hydrophilic fraction. Geochim Cosmochim Ac 2011; 75: 4005-4019.

Puy J, Galceran J, Huidobro C, Companys E, Samper N, Garcés JL, Mas F. Conditional Affinity Spectra of Pb^{2+}-Humic Acid Complexation from Data Obtained with AGNES. Environ Sci Technol 2008; 42: 9289-9295.

Zavarise F, Companys E, Galceran J, Alberti G, Profumo A. Application of the new electroanalytical technique AGNES for the determination of free Zn concentration in river water. Anal Bioanal Chem 2010; 397: 389-394.